

IMPROVEMENT DESIGN OF A BEAM CURRENT MONITOR BASED ON A PASSIVE CAVITY UNDER HEAVY HEAT LOAD AND RADIATION

P. A. Duperrex[†], J. Sun, J. E. Bachmann, M. Rohrer
Paul Scherrer Institut, 5232 Villigen PSI, Switzerland

Abstract

The High Intensity Proton Accelerator (HIPA) at PSI delivers a continuous proton beam of up to 2.4 mA with a maximum energy of 590 MeV to two meson production targets, M and E, and then to the SINQ spallation target. The scattered particles from the beam's interaction with Target E affect the performance of a resonator-based current beam monitor. To minimize these issues, a graphite monitor was designed to replace the older aluminum one.

Based on years of operating experience with this graphite cavity, improvements to the design have been considered, including refining beam position pickups, implementing online calibration methods, and addressing manipulation and maintenance issues. Detailed aspects of the monitor's performance and its improved design are presented.

INTRODUCTION

The HIPA can generate up to 1.4 MW continuous proton beam [1]. After the main cyclotron extraction, the beam is transported through a 60 m long beam line with two graphite target stations, TM and TE for Muon and Pion production. The TM has a thickness of 5 mm and absorbs ~1% of the beam. The TE is 40 mm (alternatively 60 mm) thick and absorbs ~8% (~12%) of protons. Then the remaining beam is directed to the SINQ spallation source for neutron production. Collimators or local shielding are responsible for further beam losses leading to additional ~20% (~30%) beam losses while the remaining ~72% (~58%) of protons are transmitted to the SINQ target through a 55 m beam line [2].

A proton beam current monitor, called MHC5, is located 8 meters downstream of target E in the high-energy beam line of HIPA. It is a coaxial cavity tuned to the second harmonic (101.26 MHz) of the proton beam pulse frequency. MHC5 is a key element for beam operation, as any deviation from the expected transmission from target E could damage the SINQ target.

A main concern for MHC5 is the energy deposition from the scattered particle shower due to the target E. This causes large temperature variations in the resonator, leading to resonance frequency and calibration drifts during beam operation [3].

To address this issue, an aluminum cavity with active cooling was first implemented. However, the resonance frequency shift was still too large. A later study showed that the cavity thermal gradient due to active cooling was inducing an even larger shift [4]. Therefore, materials with lower thermal expansion coefficients and higher radiation emissivity (since the resonator is in the beam line vacuum) were considered for a new MHC5 design.

[†] pierre-andre.duperrex@psi.ch

PASSIVE CAVITY MADE OF GRAPHITE

Advantages

Graphite has several advantages over aluminum for the MHC5 cavity. Its lower thermal expansion coefficient reduces thermal deformation, leading to smaller frequency drift. Its higher radiation emissivity improves cooling and reduces temperature excursions. Without active cooling, thermal gradient issues are minimized. Additionally, its lower electrical conductivity reduces the cavity's Q factor, making the resonator less sensitive to frequency drift.

Figure 1 shows the graphite cavity under laboratory test, with eight graphite screws used for fine tuning. The monitor was installed on the beam line in early 2015.

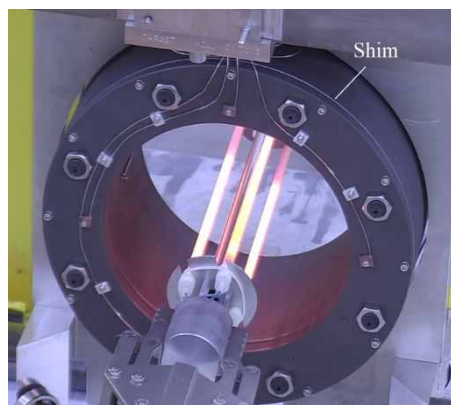


Figure 1: The graphite MHC5 being tested after maintenance in 2017, quartz tube in the center of the monitor to test the thermal load effects on the resonator the beam.

Further simulation studies show that thermal expansion always causes negative frequency drift, with a higher temperature leading to a lower resonance frequency. One possible way to counteract this effect is to use a second material with a much larger expansion coefficient to increase the capacitor gap, thereby increasing the resonance frequency. This self-compensating method was implemented by inserting a thin aluminum shim at the capacitor gap position, as shown in Fig. 1.

Performances

Figure 2 shows historical data of the MHC5 and a NPCT Bergoz [5] current monitor (MHC6B) during a service day of HIPA, with a beam intensity of up to 1800 μ A. As the Bergoz monitor performs an absolute measurement of the beam current, it can be used to calibrate the MHC5. This calibration procedure cannot be considered "online" because the Bergoz electronics must be compensated at each calibration, which requires interrupting the beam for several seconds. The MHC5 shows good linearity with the Bergoz monitor before the beam is stopped, because the

MHC5 temperature is rather stable. As the beam is stopped for several hours, the MHC5 cools down to ~ 65 °C. When the beam comes back on, the MHC5 shows a deviation ($\sim 2.5\%$) from the Bergoz monitor in the first few hours, due to the frequency drift effect related to the large temperature excursions. As the temperature stabilizes, the deviation between the MHC5 and Bergoz monitors becomes much smaller.

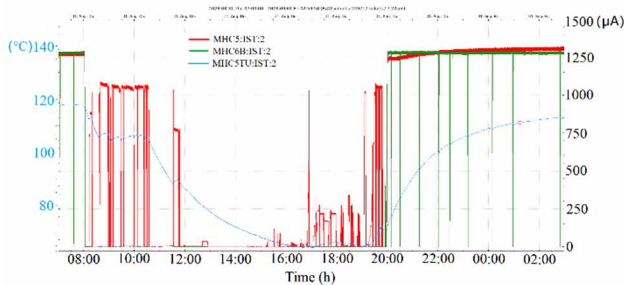


Figure 2: The MHC5 temperature (blue curve) drifting with the intensity of the beam during a service day. Beam current measured by MHC5 (red) and MHC6B (green).

ONLINE CALIBRATION

Scenario

On-line calibration of the resonator is highly desirable to improve the measurement accuracy. As already mentioned, the resonator is subject to large temperature variations and the resulting calibration changes are unavoidable. A first scheme was tested a few years ago but the method lacked of long time stabilities and was practically not usable.

The new calibration scheme is based on network analyzer measurements of the resonator transmission at frequencies off the RF frequency band (in our case 600 kHz around 101.26 MHz) to avoid interferences with the beam current measurements. The resonator gain is estimated by performing a non-linear fit of the resonance.

The Rohde & Schwarz ZN8 Network Analyzer remote control as well as the Levenberg-Marquardt (L-M) nonlinear least squares curve fitting are performed using LabVIEW on a Windows PC. The fitting of the resonance amplitude function [6]

$$\|S_{21}(f)\| = \frac{\bar{S}_{12}}{\sqrt{1 + \left(Q \left(\frac{f}{f_0} - \frac{f_0}{f}\right)\right)^2}} \quad (1)$$

provides the f_0 , Q and \bar{S}_{21} estimate for the calculation of the gain at the RF frequency. The standard deviations σ_{f_0} , σ_Q and $\sigma_{\bar{S}_{21}}$ is derived from the L-M fit covariance matrix. The estimated error on the resonator gain measurements is then performed using the error propagation equation for the uncorrelated variables f_0 , Q and \bar{S}_{21} [7]:

$$\sigma_{\|S_{21}\|}^2 = \left(\frac{\partial \|S_{21}\|}{\partial f_0}\right)^2 \sigma_{f_0}^2 + \left(\frac{\partial \|S_{21}\|}{\partial Q}\right)^2 \sigma_Q^2 + \left(\frac{\partial \|S_{21}\|}{\partial \bar{S}_{21}}\right)^2 \sigma_{\bar{S}_{21}}^2 \quad (2)$$

Results

Example of such analysis is shown in Fig.3. It presents the measured transmission and the fitting for a beam current of 1.277 mA and a resonator temperature of 116 °C. From the fitted values $f_0 = 101.07$ MHz, $Q = 74.0755$ and $\bar{S}_{21} = 0.0411$, the MHC5 gain (S_{21} at 101.26 MHz) is 0.0396 with a relative standard deviation of $\sim 2 \times 10^{-3}$.

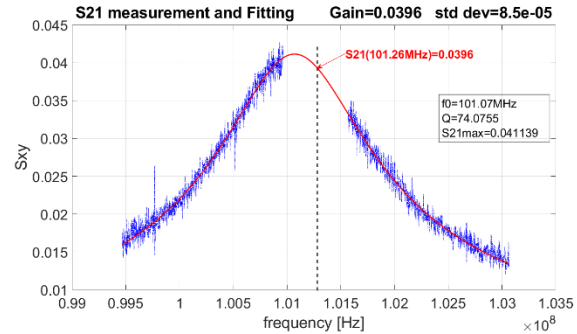


Figure 3: Example of transmission measurements (blue line) and fitting (red line).

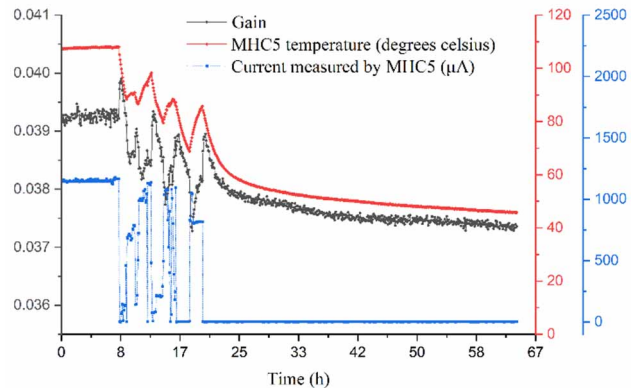


Figure 4: Gain, temperature and beam intensity as measured with the MHC5 during a cooling phase.

Figure 4 shows an example of the time evolution of the fitted gain along the beam current intensity and the resonator temperature. The gain is observed to drop from a maximum value of 0.4 to 0.374 ($\sim 7\%$ variation) for no beam. The temperature variations due to the modulation of beam intensity are clearly visible as well as the cooling phase in absence of beam. The gain behaviours during these strong temperature variations is more complex and shows some transient effects. At each change of the thermal load, the parameter changes are observed first to go in the other direction from the expected one. This effect may be attributed to the fact that, since the radiation cooling originates from the external surfaces of the resonator and the thermal load is more a volume effect, stronger temperature gradients and resulting mechanical stresses are then expected at the initial phase. This is leading to an additional drift of the gain. These effects also explain why it was not possible to directly relate the temperature to the gain value for beam operation.

DESIGN IMPROVEMENT OF THE BEAM POSITION PICKUPS

Inductive Pickups of the System in Operation

Grooves with 5 mm radius and 100 mm length were milled at the inner surface of the MHC5, to mount 4 inductive pick-ups providing an additional BPM measurements capability of the system (Fig. 5).

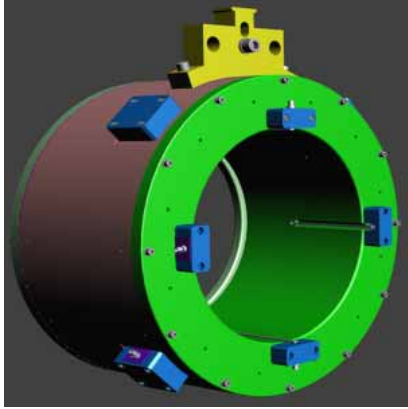


Figure 5: Four inductive beam position pickups located on the beam entry side of MHC5.

BPM Tests with Beam

Since the BPM measurements are not yet implemented in the control system, these tests were performed using a portable spectrum analyzer (Fieldfox N9913A from Agilent Technologies) for different beam intensities and positions. As expected, the sum of the 4 pickup signals is observed (see Fig.6) to be directly proportional to the beam current (measured by MHC4, a beam current monitor located before TE). The small positive offset for no beam (intercept of the calculated linear regression) can be attributed to the instrumental noise. These results confirm its potential use as additional beam current measurement. Further studies are needed to quantify the temperature induced drifts but, since there are broadband measurements, there are expected to be smaller than the cavity measurements.

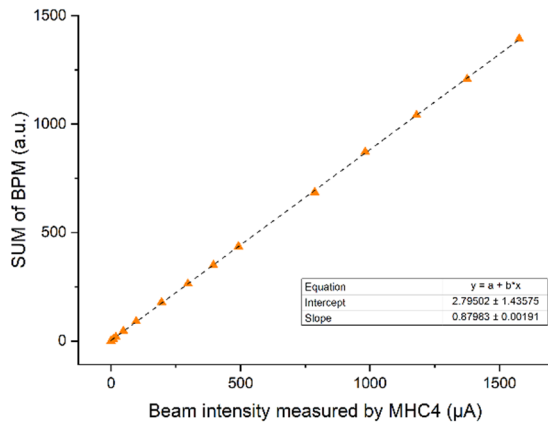


Figure 6: Sum of the position pickups in respect to the beam intensity measured by MHC4.

A wire scanner (MHP41) mounted just behind the MHC5 was used as reference for the beam horizontal position scanning. The (Right-Left)/Sum value shows a good linearity with respect to the MHP41 (see Fig. 7).

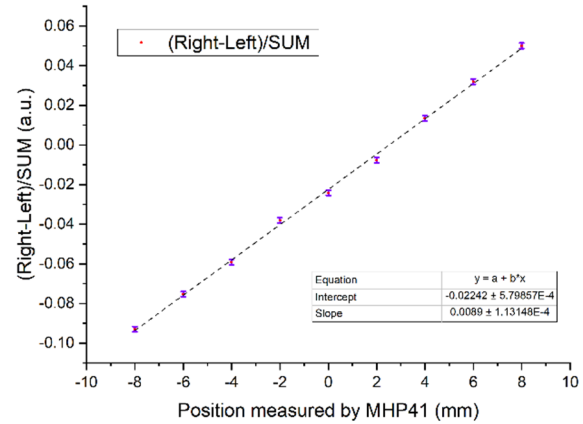


Figure 7: The diff/sum calculation with respect to the beam position measured by MHP41.

Capacitive Pickups for the New System

The new design incorporates a major improvement by increasing the number of pickups to eight. This enhancement will improve not only the intensity and position measurements, but will also provide an ellipticity estimate.

In addition, the possibility to measure the bunch length was also investigated for the upgrade design. That requires a shorter pickup to have a better time domain response. However, for the inductive solution, the signal level would decrease significantly. Thus, a new design with capacitive pickups, or buttons, was setup and simulated by CST [8].

The pickup signal is the sum of the mirror charges on the pickup plate [8].

$$i_{\text{pickup}} = \int_{(-L/2)/\beta c}^{(+L/2)/\beta c} \frac{d}{dt} i_b(t) dt \frac{Arc_{\text{pickup}}}{Circum_{\text{pipe}}} \quad (3)$$

where Arc_{pickup} is the radial aperture of the electrode expressed in units of length and L the button length. In the case of pickup length $L \ll$ bunch length, the pickup signal is the time derivative of the image charge distribution.

The pickup response to a 590 MeV single proton bunch ($\sigma_{\text{beam}} = 43$ mm) has been calculated using CST for different configurations. As an example, the pickup signal for various pickup angle apertures (length fixed at 17 mm) is shown in Fig. 8.

Because of the β effect, the image charge distribution is wider than the physical length of the bunch and the length of the image charge of the bunch can be given by [9]:

$$\sigma_{\text{im}} = \sqrt{\sigma_s^2 + \sigma_{\text{beam}}^2} \quad (4)$$

where σ_{im} is the rms length of the image charge on the beam pipe, $\sigma_s = a/\gamma\sqrt{2}$ is the rms length of the electrical field created by a single charged particle moving at βc , γ is the relativist factor and a is the pipe radius, σ_{beam} is the rms

length of the bunch. Thus, the bunch length can be calculated out with Eq. (4) from the measured pickup signal. In our case, $\sigma_s = 60.7$ mm and $\sigma_{\text{beam}} \approx 43$ mm so $\sigma_{\text{im}} \approx 74.4$ mm.

With $\beta = 0.79$, we get $\sigma_{\text{im}} \approx 0.63$ ns which is consistent with the peak-to-peak width of simulated pulse (see Fig.8).

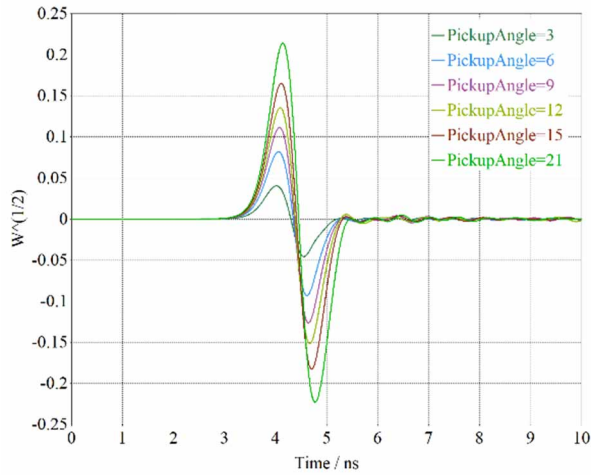


Figure 8: The pickup response to a Gaussian shaped proton pulse for different angle apertures. The signal amplitude is proportional to the angle aperture (button size effect).

The beam position derived from the difference over sum calculation of the simulated pickup signals (pickup dimensions: 12 degrees aperture and $l = 17$ mm) for different beam positions is shown in Fig. 9. The results are typical for such calculations, the sensitivity of the measurements decreasing for large off-center conditions.

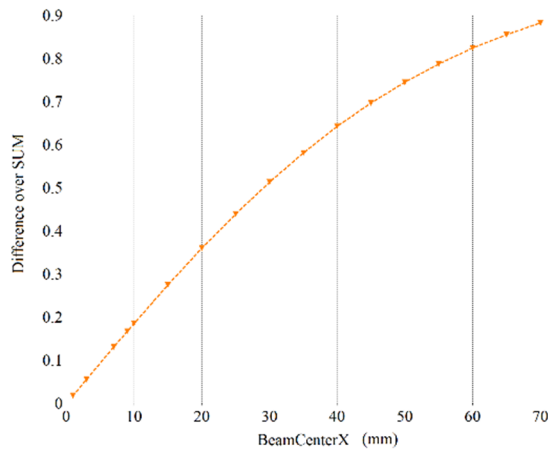


Figure 9: Diff/Sum response for various beam off-center positions of the new capacitive version of the BPM.

IMPROVED MAINTENANCE FEATURES

The MHC5 is operating in an extremely high radiation area, hanging under a 2.5m long bulky steel shielding in the beam bunker. In the past, the whole shield had to be replaced for a new resonator installation. To minimize the radioactive wastes, the new modular design (see Fig. 10 left) allows the upper segments to be re-used in case of monitor failure.

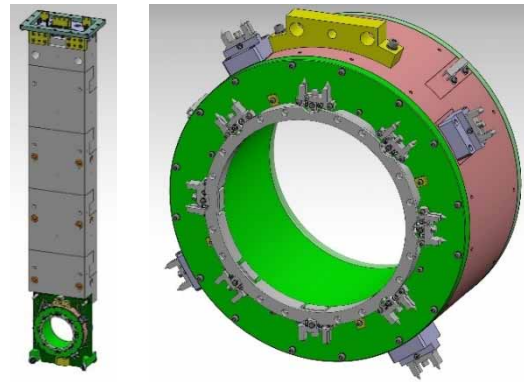


Figure 10: Overview of the improvement design of the MHC5 and its shielding (left); Details of the new MHC5 (right) with the 8 BPM buttons and the 4 ports for the resonance measurements and tests.

Remote Maintenance

To minimize the human exposure to radiations in case of repairs of maintenance, a PSI solution was specially developed for the cable plugin/out to the pickups allowing the use of manipulators (Fig. 10 right). To facilitate the manipulator operations, the semi-rigid cable used in the previous systems are replaced in the new version by Kapton cables

CONCLUSION

The graphite version of the MHC5 has been successfully operated under heavy heat load and radiation since 2015 and the beam position pickups perform as expected. The on-line calibration method improves further the stability of the measurements. The new MHC5 design will further broaden the type of measurements performed, facilitate maintenance, minimize human radiation exposures and active wastes in case of replacement. Lab tests with the new system are expected to take place beginning of next year.

REFERENCES

- [1] M. Seidel *et al.*, “Production of a 1.3 MW proton beam at PSI”, in *Proc. 1st Int. Particle Accelerator Conf. (IPAC’10)*, Kyoto, Japan, May 2010, pp. 1309–1313.
- [2] D. Reggiani *et al.*, “Improving machine and target protection in the SINQ beam line at PSI-HIPA”, in *Proc. 9th Int. Particle Accelerator Conf. (IPAC’18)*, Vancouver, BC, Canada, Apr.-May 2018, pp. 2337-2340. doi:10.18429/JACoW-IPAC2018-WEPAL068
- [3] P. A. Duperrex *et al.*, “New on-line gain drift compensation for resonant current monitor under heavy heat load”, in *Proc. 1st Int. Particle Accelerator Conf. (IPAC’10)*, Kyoto, Japan, May 2010, pp. 1122–1124.
- [4] J. Sun *et al.*, “Design of a new beam current monitor under heavy head load”, in *Proc. 54th ICFA Advanced Beam Dynamics Workshop on High-Intensity, High Brightness and High Power Hadron Beams (HB’14)*, East-Lansing, MI, USA, Nov. 2014, pp. 154-156.
- [5] Bergoz NPCT, <https://www.bergoz.com/products/npct/>

- [6] P. J. Petersan and S. M. Anlage, "Measurement of resonant frequency and quality factor of microwave resonators: Comparison of methods", *J. Appl. Phys.*, vol. 84, pp. 3392-3402, 1998. doi:10.1063/1.368498
- [7] J. Tellinghuisen, "Statistical error propagation", *J. Phys. Chem. A*, vol. 105, no.15, pp. 3917-3921, 2001. doi:10.1021/jp003484u
- [8] CST Studio Suite, <https://www.3ds.com/products-services/simulia/products/cst-studio-suite/>
- [9] M. Cohen-Solal, "Design, test, and calibration of an electrostatic beam position monitor", *Phys. Rev. Spec. Top. Accel. Beams*, vol. 13, p. 032801, 2010. doi:10.1103/PhysRevSTAB.13.032801